Measurement 145 (2019) 130–136

Contents lists available at ScienceDirect

Measurement

journal homepage: www.elsevier.com/locate/measurement

Estimation of angular velocity and acceleration with Kalman filter, based on position measurement only

Johnny Rodriguez-Maldonado

State University of Nuevo Leon, (UANL), Pedro de Alba s/n, San Nicolas de Los Garza, Nuevo Leon 66455, Mexico

ARTICLE INFO

Article history:
Received 30 October 2018
Received in revised form 2 May 2019
Accepted 11 May 2019
Available online 18 May 2019

Keywords:
Tracking filter
Velocity estimation
Taylor Kalman filter
Digital differentiator
Acceleration estimation

ABSTRACT

This paper presents a method to obtain good synchronous and instantaneous estimates in position, velocity and acceleration; using a position measurement only. The proposed method shows better estimates in position, velocity and acceleration than other methods such as nonlinear tracking differentiator (TD), extended state estimation (ESO) and digital differentiator based on Taylor series (DDBTS). The proposed method allows for an increased accuracy of estimates by generating a feedback frequency obtained to the position measurement signals. The model and method proposed in this paper reduce the error when the measurement signal presents a change in frequency. The model update and adjusts simultaneously to changes in sample rates using a feedback frequency estimate. The proposed method was validated with the QNET DC Motor Control Trained (DCMCT). Since the method requires the measurement position only from an encoder, it eliminates the need for more sensors for velocity and acceleration, thus begin less costly.

1. Introduction

Nowadays in many applications as robotics, monitoring by GPS, control motors, controlled motion systems, and others, the information as position, velocity, and acceleration are very important. This information provided by the monitoring of the systems is crucial to make a decision or control of the systems. For example, the measurement of position in the displacement is crucial, as is demonstrated in [1] where is measurement the displacement for understanding and characterizing the behavior of civil infrastructure using an RTK-GPS. But in the application are used three sensors to obtain the estimates of displacement, velocity an acceleration. Another application that considered the velocity change to designing the control strategy for the connected cruise control is presented in [2]. The track condition monitoring based on the bogie and car body acceleration measurement is presented in [3] using a mathematical model. The disadvantage to used a model, is that in some systems is very difficult or imprecise the estimation of the model.

One of the most used sensor to obtain the signal position in electrical motors is the encoder. Some estimations of angular velocity based in the measured position are presented in [4–8]; unfortunately, most of these are unsatisfactory in control applications due to the delay that is inherited in the derivative estimates provided by this filters, that produce adverse effects in stability [9]. As an alternative, some methods employ a Kalman filter to estimate the velocity. However, the Kalman filter model presented in [10–12] requires a target velocity trajectory.

In [13] is proposed an adaptive model-free observer for robot manipulators in the task-space without the use of task-space velocity measurement. Also in [14] are used a combination of an accelerometer and an encoder to estimate velocity, using an observer, the application is considering a robot performing in rigid contact modeling and control. In the sense of the fault detection, was proposed in [15] an algorithm extract the features of helical gear fault, using an optimal encoder and tracking analysis based on the angular domain asynchronous averaging. In [16] was proposed a finite-response filter with adaptive window length to estimate position and velocity, the estimates are concentrated in velocity jump, the precision in its estimates have a threshold that depends to the sampling position data and predicted position, one advantage of the method is that not need a system model. On the other hand, the comparison study between different velocity and acceleration estimators are presented in [17] using an encoder to measure position.

The model used in [11,17–19] estimate the angular velocity and angular acceleration with the Kalman filter, but this model requires a constant sampling interval obtained through the encoder system with an interpulse angle. Another method that needs a constant sampling interval is presented in [4]. A disadvantage

E-mail address: johnny.rodriguezml@uanl.edu.mx

https://doi.org/10.1016/j.measurement.2019.05.043
0263-2241/

to these methods is that there considered a constant frequency that is implemented in its model. Thus the estimates become significantly degraded as a sampling rates increase or the measurement signal present dynamical changes in its frequency.

The main idea of this paper is to use of the Kalman filter with a model that is able to obtain instantaneous estimates in position, velocity, and acceleration at the same time (synchronous), using the measurement position only. Also as the proposed model used a dynamical frequency that is estimated with another model presented in [20] and then is implemented in the model that is presented in this work, and so, both models developed the proposed algorithm to estimate the position, velocity, and acceleration. As the proposed Kalman differentiator uses an update frequency, the method is effective in low-speed and high-speed ranges. Therefore is able to provide better instantaneous derivatives estimates than other methods as nonlinear tracking differentiator (TD) [21–23], the extended state observer (ESO) presented in [24,25] and the digital differentiator based on Taylor series (DDBTS) that is another common differentiator [26].

On the other hand, as the proposed Kalman Differentiator (KD) filter is based on an analytic function that is defined as an exponential function with angular frequency. The model used a frequency that in its first stage are proposed as initial conditions and then is estimated by the measurement signal, and so the frequency updates to the model. Thus, the KD obtain better estimates when the measurement signals have a dynamic frequency.

This paper is organized as follows. Section 2 presents the model to obtain the dynamic frequency estimate, using the position measurement. Section 3 establishes the design of the state space signal model with its transition matrix and the Kalman filter equation. Finally, the position, velocity and acceleration estimates are presented in Section 4.

2. Frequency estimation

In [20] was developed a model that is implemented in Kalman filter to obtain the phasor and frequency estimates. The signal model is defined as

$$s(t) = \Re\{p(t)e^{j\omega_1 t}\} = \Re\{r(t)\}, \tag{1}$$

where $p(t) = a(t)e^{j\varphi(t)}$ is the phasor, $a(t)$ and $\varphi(t)$ the amplitude and phase respectively. Also with a transition matrix $\boldsymbol{\Psi}_K(\tau) = \boldsymbol{M_K}\boldsymbol{\Phi_K}(\tau)\boldsymbol{M_K^{-1}}$ where

$$\boldsymbol{\Phi}_K(\tau) = \begin{pmatrix} 1 & \tau & \frac{\tau^2}{2!} & \dots & \frac{\tau^K}{K!} \\ & 1 & \tau & \dots & \frac{\tau^{K-1}}{(K-1)!} \\ & & 1 & \dots & \frac{\tau^{K-2}}{(K-2)!} \\ & & & \ddots & \vdots \\ & & & & 1 \end{pmatrix}, \tag{2}$$

and with an invertible matrix, where the row p and columns q of the matrix $\boldsymbol{M}_K$, are obtained by

$$m_{pq} = \begin{cases} \binom{p-1}{q-1}(j\omega)^{p-q}, & p \geqslant q. \\ 0, & p < q. \end{cases} \tag{3}$$

On the other hand the discrete state space model is defined

$$\boldsymbol{x}[n] = \boldsymbol{A}\boldsymbol{x}[n-1] + \boldsymbol{F}\boldsymbol{v}[\boldsymbol{n}] \tag{4}$$

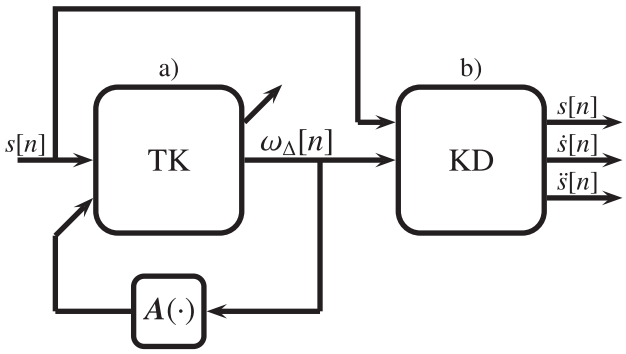

Fig. 1. Block diagram describing the sequence to estimate position, velocity and acceleration.

with

$$\boldsymbol{A} = \begin{bmatrix} e^{j\omega_1\tau}\boldsymbol{\Psi}_K(\tau) & \\ & e^{-j\omega_1\tau}\overline{\boldsymbol{\Psi}}_K(\tau) \end{bmatrix}. \tag{5}$$

The measurement equation, that is the truncated signal model is given by

$$y[n] = \boldsymbol{H}\boldsymbol{x}[n] \tag{6}$$

where $\boldsymbol{H} = \frac{1}{2}\left[\boldsymbol{h}^T\boldsymbol{h}^T\right]$ and $\boldsymbol{h} = [1 \quad 0 \quad \dots \quad 0] \in \mathbb{R}^{1\times(K+1)}$.

On the other hand, note that all matrices and parameters of this Section 2 are defined at the first stage and then are implemented successively, for more details it can be seen the next subSection 3.3 and Fig. 1. Note that the development of this Section 2 in the Fig. 1 is called Taylor Kalman (TK) filter. The proposed methodology to estimate the position, velocity and acceleration, are presented in the next section.

3. Proposed methodology

In this section its shown the development of two models for KD (see subSections 3.1 and 3.2) and the procedure to obtain estimations in position, velocity and acceleration.

3.1. Dynamical model I

We can start with a signal model $s(t)$ that is defined by analytic function

$$s(t) = e^{j\omega t} \tag{7}$$

and it can be approximated by Taylor series centered in t_0

$$s(t) = \sum_{K=0}^{\infty} \frac{s^{(K)}(t_0)}{K!}(t - to)^K. \tag{8}$$

Hence the derivative of (8) is given by

$$s_K^{(1)}(t) = s(t_0)(j\omega) + s^{(1)}(t_0)[(j\omega)\tau + 1] + \dots + s^{(K)}(t_0)\left[(j\omega)\frac{\tau^K}{K!} + \frac{\tau^{K-1}}{(K-1)!}\right] \tag{9}$$

and the second derivative

$$s_K^{(2)}(t) = s(t_0)(j\omega)^2 + s^{(1)}(t_0)\left[(j\omega)^2\tau + 2j\omega\right] + \dots + s^{(K)}(t_0)\left[(j\omega)^2\frac{\tau^K}{K!} + (2j\omega)\frac{\tau^{K-1}}{(K-1)!} + \tau\right] \tag{10}$$

where $\tau = t - t_0$.

Additionally, the Kth derivative of (8) is obtained as

$$\begin{aligned} s_K^{(K)}(t) = s(t_0)(j\omega)^K + s^{(1)}(t_0)\left[(j\omega)^K\tau + K(j\omega)^{(K-1)}\right] \\ +s^{(2)}(t_0)\left[(j\omega)^K\tfrac{\tau^2}{2!} + K(j\omega)^{(K-1)}\tau + K(K-1)j\omega\right] \\ \vdots \\ +s^{(K)}(t_0)\left[(j\omega)^K\tfrac{\tau^K}{K!} + K(j\omega)^{(K-1)}\left(\tfrac{\tau^{(K-1)}}{(K-1)!}\right) + \ldots + 1\right] \end{aligned}$$

Finally, the transition matrix it can be defined as shown in (11),

$$\boldsymbol{\Lambda}_K(\tau) = \begin{pmatrix} \lambda_{1,1} & \lambda_{1,2} & \lambda_{1,3} & \ldots & \lambda_{1,K} \\ \lambda_{2,1} & \lambda_{2,2} & \lambda_{2,3} & \ldots & \lambda_{2,K} \\ \lambda_{3,1} & \lambda_{3,2} & \lambda_{3,3} & \ldots & \lambda_{3,K} \\ \vdots & \vdots & \vdots & \ddots & \vdots \\ \lambda_{K,1} & \lambda_{K,2} & \lambda_{K,3} & \ldots & \lambda_{K,K} \end{pmatrix} \tag{11}$$

the elements of (11) are shown in the appendix. Note that rows are the successive derivatives of the analytic signal function.

The steady state vector is $\boldsymbol{s_K}(\boldsymbol{t})$, it can be rewritten as

$$\boldsymbol{s_K}(\boldsymbol{t}) = \boldsymbol{\Lambda_K}(\tau)\boldsymbol{s}(\boldsymbol{t_0}). \tag{12}$$

The steady state in the discrete form it can be obtained assuming $t_0 = (n-1)\tau, t = n\tau$, and τ is sampling period. Also note that $\omega = 2\pi f_1\tau$, hence $\omega = 2\pi/N_1$ where N_1 is the number of samples. Therefore the signal model is given by

$$\boldsymbol{s_K}[\boldsymbol{n}] = \boldsymbol{\Lambda_K}(\tau)\boldsymbol{s}[\boldsymbol{n}-\boldsymbol{1}], \tag{13}$$

the vector $\boldsymbol{s_K}[\boldsymbol{n}]$ have the position and its successive derivatives. To obtain the correct amplitude in derivatives is necessary

$$\boldsymbol{\chi}_K[n] = \left[s[n]_K \quad s[n]_K^{(1)}\tau \quad s[n]_K^{(2)}\frac{\tau^2}{2!} \quad \ldots \quad s[n]_K^{(K)}\frac{\tau^K}{K!}\right]^T \tag{14}$$

Note that the observation (or measurement) model now is

$$s_K[n] = \boldsymbol{h}\boldsymbol{\chi}_K[n] \tag{15}$$

where $\boldsymbol{h} = [1\ 0\ \ldots\ 0] \in \mathbb{R}^{1\times(K+1)}$.

As the phasor estimates and its derivatives can be obtained from the TK estimates, the frequency it could be updated at each iteration, from the TK estimates through

$$\omega_\Delta[n] = \frac{Im\{\dot{p}_K[n]e^{-j\measuredangle p_K[n]}\}}{|p_K[n]|}, \tag{16}$$

The existence of frequency estimates (16), and a transition matrix dependent form the frequency (5) lead us to propose the use of the following time variant transition matrix:

$$\boldsymbol{\Lambda}[n] = \begin{pmatrix} e^{j\omega[n]\tau}\boldsymbol{\Psi}_K(\tau,\omega[n]) & \\ & e^{-j\omega[n]\tau}\overline{\boldsymbol{\Psi}}_K(\tau,\omega[n]) \end{pmatrix}, \tag{17}$$

with

$$\omega[n] = g\{\omega[n-1], \Delta_\omega[n-1]\}, \tag{18}$$

where the function g denotes the adaptation rule, and it is such that a correct tracking of the frequency is performed.

3.2. Dynamical Model II

The second model considers the derivatives in the vector $\boldsymbol{s_K}[\boldsymbol{n}]$, and thus is obtain the measurement signal model as

$$s_K[n] = \boldsymbol{h}_2\boldsymbol{\chi}_K[n] \tag{19}$$

where $\boldsymbol{h}_2 = \begin{bmatrix}1 & j\omega & (j\omega)^2 & \ldots & (j\omega)^K\end{bmatrix}$, therefore the next convergence power series is obtained

$$s_K[n] = \sum_{K=0}^{\infty}(j\omega)^K s[n]^{(K)}\frac{\tau^K}{K!} \tag{20}$$

where K in $s[n]$ represents the number of derivatives.

3.3. The auto recursive process

The implementation filter is defined by the following sequence:

1. Time update:
   (a) State prediction

$$\boldsymbol{\Lambda}_K[n] = \boldsymbol{\Lambda}_K[n-1] \tag{21}$$

$$\hat{\boldsymbol{x}}^-[n] = \boldsymbol{\Lambda}_K[n]\hat{\boldsymbol{x}}[n-1] + \boldsymbol{F}_K\sigma_w^2[n] \tag{22}$$

   (b) A *priori* error covariance

$$\boldsymbol{P}^-[n] = \boldsymbol{\Lambda}_K[n]\boldsymbol{P}[n-1]\boldsymbol{\Lambda}_K^H[n] + \boldsymbol{\Gamma}\boldsymbol{\Gamma}^T\sigma_v^2 \tag{23}$$

2. Measurement update
   (a) Kalman gain:

$$\boldsymbol{K}[n] = \boldsymbol{P}^-[n]\boldsymbol{h}^T\left(\boldsymbol{h}\boldsymbol{P}^-[n]\boldsymbol{h}^T + \sigma_w^2\right)^{-1} \tag{24}$$

   (b) State update

$$\hat{\boldsymbol{x}}[n] = \hat{\boldsymbol{x}}^-[n] + \boldsymbol{K}[n](s[n] - \boldsymbol{h}\hat{\boldsymbol{x}}[n]) \tag{25}$$

   (c) A posteriori error covariance

$$\boldsymbol{P}[n] = (\boldsymbol{I} - \boldsymbol{K}[n]\boldsymbol{h})\boldsymbol{P}^-[n] \tag{26}$$

   (d) innovation measurement noise

$$\boldsymbol{\Gamma}_K\sigma_w^2[n] = s[n] - \boldsymbol{h}\hat{\boldsymbol{x}}[n] \tag{27}$$

   (e) Feedback frequency and phase (adaptive parameters). The time and measurement update equations are implemented again but with the model and matrices developed in Section 2 by frequency estimate. Then we have the phasor estimates and its derivatives, with phasor and its first derivative estimate is possible to estimate the frequency as

   i. Adaptive frequency

$$\omega_\Delta[n] = \frac{Im\left\{p_k^{(1)}[n]e^{-j\measuredangle p_k^{(0)}[n]}\right\}}{|p_k^{(0)}[n]|} \tag{28}$$

   Note that $p_k^{(0)}[n]$ and $p_k^{(1)}[n]$ are into $\hat{\boldsymbol{x}}[n]$.

   (f) Update Frequency

$$\omega[n] = i2\pi(f_1 + \omega_\Delta[n]) \tag{29}$$

   (g) Update of the dynamic state transition matrix

$$\boldsymbol{\Lambda}_K[n] = \boldsymbol{\Lambda}(\tau,\omega[n]) \tag{30}$$

where σ_v^2 and σ_w^2 are the variances of the input and measurement noise, $\boldsymbol{\Gamma} = [1 \quad 1 \quad \cdots \quad 1]^T \in \mathbb{R}^{(K+1)\times 1}$.

The process to estimate the measurements of position, velocity and acceleration are shown in Fig. 1. The algorithm consists of two sections. The first (a), consists in the frequency estimation with TK filter, that is used in the second section (b), where are obtained the estimates in position, velocity and acceleration with the KD. The

input signal is implemented in the two sections at the same time to achieved the corresponding estimates. The feedback frequency $\omega_{\triangle}$ in section (a) is implemented in the transition matrix $A(\cdot)$ to refresh the parameters in the TK filter.

4. Numerical results

4.1. Signal test

As the frequency is required in (11) and is used in the two proposed models. Then, the frequency ω is set as initial conditions as $\omega = 2\pi f_1$, where $T_1 = 1/f_1$ is the fundamental period with $N_1 = 64$ samples in this measurement signal test. Then $\omega = 2\pi/(\tau N_1)$, where the sampling period is defined as $\tau = T_1/N_1$ with $T_1 = 201.06$, that is used as initial conditions. After that, the frequency ω is estimated as can be seen in Section 3.3.

The first signal tests and its derivatives are defined as

$$s(t) = sin(sin(t)\cdot t) \tag{31}$$

$$\dot{s}(t) = [(t\cdot cos(t)) + sin(t)]\cdot cos(t\cdot sin(t)) \tag{32}$$

$$\ddot{s}(t) = (-t\cdot sin(t) + 2\cdot cos(t))\cdot cos(t\cdot sin(t)) - (t\cdot cos(t) + sin(t))^2 \cdot sin(t\cdot sin(t)) \tag{33}$$

and the following parameters in the variances for the process and measurement noise: $\sigma_v^2 = 10^{-6}\boldsymbol{I}$ and $\sigma_w^2 = 10^{-4}$ according to an SNR = 37 dB.

The parameters for TD are as follows: with a velocity factor $\delta_0 = 90$ and filtering factor to cancel out noise $h_0 = 2/N_1$, for ESO are $\delta = 0.01, \alpha = 0.5, \beta = 50, \beta_2 = 150$ and $\beta_3 = 50$, the implementation and equations it can be seen in [27].

As can be seen in Fig. 2, the proposed Kalman derivative algorithm (KD_1, KD_2 for the proposed model *I* and model *II* respectively) provides better signal estimates than TD and ESO. DDBTS does not generate signal estimates but only derivatives of the signal. Also, when the oscillations of the signal velocity are faster, this occurs between 8 and 10 s, the estimates with TD, ESO and DDBTS produces considerable errors, as illustrated in the velocity error. The acceleration error presents a similar behavior. The acceleration estimates with DDBTS are not synchronous because the acceleration estimate presents a delay with respect to the velocity estimates.

4.2. Experimental results

The next signal test is a real measurement signal taken from QNET DC Motor Control Trainer (DCMCT), see Fig. 3. The components that comprise the DCMCT are DC motor, high-resolution encoder (0.25 deg/count), motor metal chamber and tachometer (2987 rpm/v). The measurement signal was sampled at 100 samples. The estimates and measurement of the position are shown in Fig. 4.

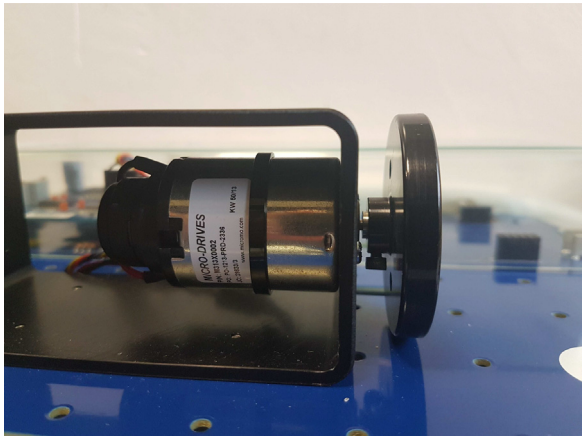

Fig. 3. Motor used for taken the measurement rotor position and velocity.

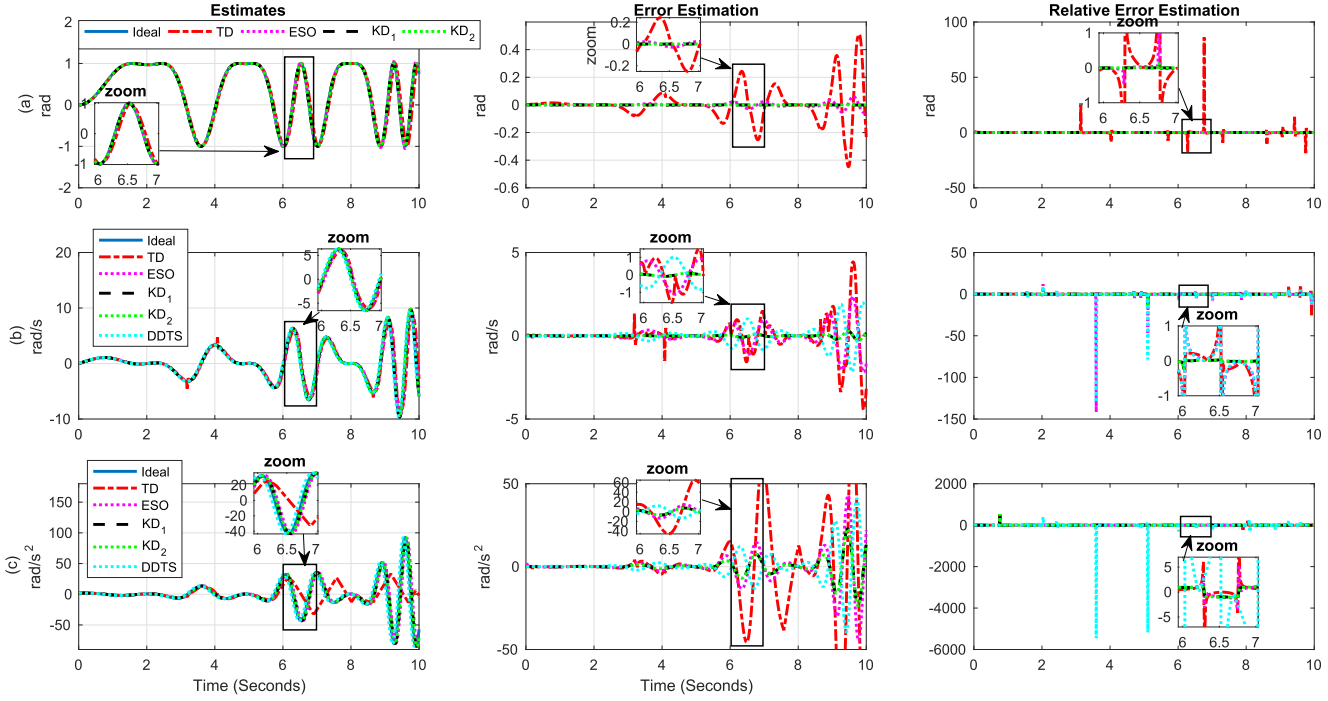

Fig. 2. (a) Position, (b) velocity, (c) acceleration and its estimation error in right column, obtained with TD, ESO, KD_1, KD_2 and DDBTS for the first signal test. With DDBTS it is not possible to estimate the signal, only its derivatives.

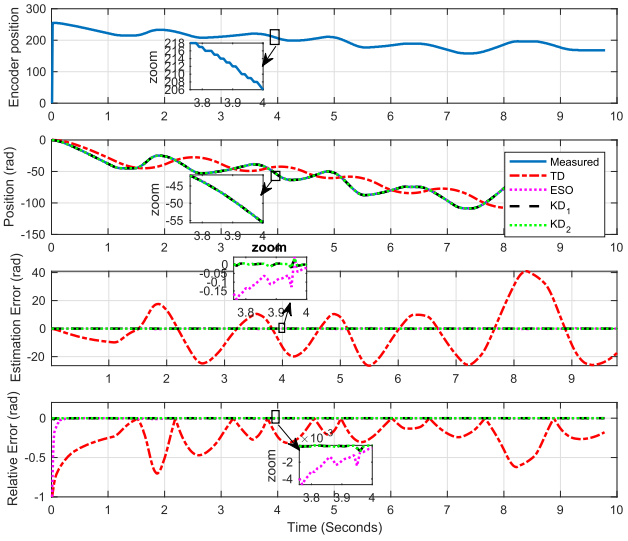

Fig. 4. Data acquisition of the position with smooth changes by QNET DCMCT, and its estimates with: TD, ESO, KD_1, and KD_2.

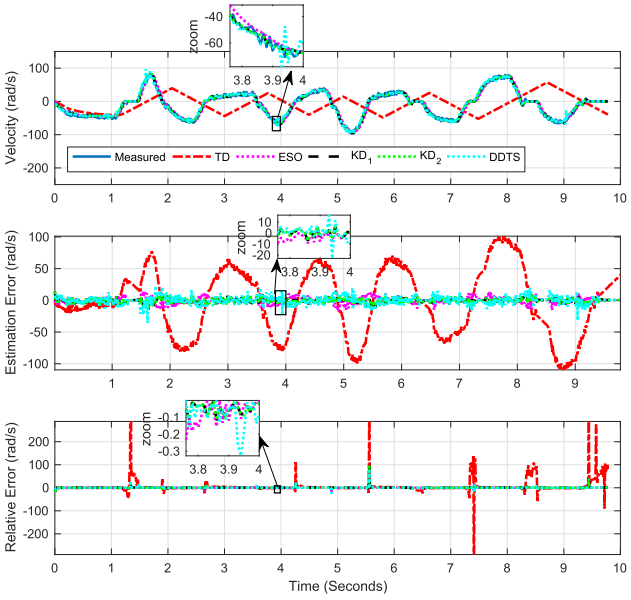

Fig. 5. Data acquisition of the rotor velocity by QNET DCMCT, (respect to Fig. 4) and its estimates with: TD, ESO, KD_1, KD_2, and DDBTS.

Again, as it can be seen in Fig. 4, the most accurate estimates are obtained with KD_1 and KD_2. The largest error is in the estimate with the TD, followed by ESO. As can be seen in the position error and it can be confirmed in Table 1, 2^{nd} signal. The estimates in velocity in Fig. 5, apparently are adequate, yet in the velocity error graph, except for TD, the estimates with TD, ESO and DDBTS are poor when compared to the KD_1 and KD_2, and it can be confirmed in Table 1, 2^{nd} signal. On the other hand, the acceleration cannot be estimated synchronously with TD, ESO and DDBTS because it is necessary to take the velocity as the new input signal to provide the estimates in acceleration, and thus a delay of one sample is generated. However, KD_1 and KD_2 with the same input signal (Position) it is possible to obtain synchronous estimates in velocity and acceleration.

The simulated and real measurement signals illustrated in Fig. 2 and 4 respectively, present smooth changes in position. The better estimates of the signals are obtained with the KD_1 and KD_2. Also, the results of the comparison methods it can be seen in Table 1$2^{nd}$ Signal, where it can be confirmed the percent error at each method.

Another kind of proof is a measurement signal provided by the DCMCT. Where the movement (position) of the rotor, present abrupt changes between -2π and 2π. The estimations are illustrated in Fig. 6 and Fig. 7 by position and velocity respectively. The percent error by this signal in Table 1 it can be found in 3^{rd} Signal. In this case, the better estimates in position are obtained with KD_1 and KD_2, using a variance $\sigma_w^2 = 10^{-5}$. Unfortunately, the estimates in velocity, not present the better estimates with KD_1 and KD_2. But with $\sigma_w^2 = 10^{-3}$, the percent error in velocity is 4.016 that achieved better estimates in 3^{rd} signal than the other methods. To obtain, satisfactory parameters with Kalman filter is necessary an appropriate representation of the process and measurement noises with zero-mean noises. However, in [28] was presented with a recursive method that switches between two models depending on whether the system is in steady-state or transient. Such that adjust the value of covariance noise in Kalman filter. It could be an alternative to achieved better estimates, but the study of the noise is not the aim of this work. On the other hand, the control

Table 1
Percent error estimates. The 1^{st} signal test is defined by Eqs. (35)–(37) by position (s), velocity ($\dot{s}$) and acceleration ($\ddot{s}$) respectively. The position and velocity errors by signals 2^{nd} and 3^{rd} are with respect to the encoder a tachometer signal respectively, that are included in the QNET DCMCT system. Thence that the acceleration column is empty.

Signal	Differentiators	s (Position)				$\dot{s}$ (Velocity)				$\ddot{s}$ (acceleration)			
			Noise response for KD (σ_w^2)				Noise response for KD (σ_w^2)				Noise response for KD (σ_w^2)		
			10^{-5}	10^{-4}	10^{-3}		10^{-5}	10^{-4}	10^{-3}		10^{-5}	10^{-4}	10^{-3}
1st Signal	TD	0.262	–	–	–	1.32	–	–	–	686.21	–	–	–
	ESO	0.041	–	–	–	0.713	–	–	–	245.59	–	–	–
	DDBTS	–	–	–	–	1.003	–	–	–	223.02	–	–	–
	KD_1	–	$9.64e-05$	$5.712e-04$	0.002	–	0.086	0.199	0.487	–	90.24	130.59	196.73
	KD_2	–	$9.64e-05$	$5.712e-04$	0.002	–	0.086	0.199	0.487	–	90.24	130.59	196.73
2nd Signal	TD	−20.723	–	–	–	−28.341	–	–	–	–	–	–	–
	ESO	−0.120	–	–	–	−2.164	–	–	–	–	–	–	–
	DDBTS	–	–	–	–	−2.524	–	–	–	–	–	–	–
	KD_1	–	$-16e-04$	−0.003	−0.008	–	−1.734	−1.581	−1.451	–	–	–	–
	KD_2	–	$-16e-04$	−0.003	−0.008	–	−1.734	−1.581	−1.451	–	–	–	–
3rd Signal	TD	0.358	–	–	–	8.684	–	–	–	–	–	–	–
	ESO	0.078	–	–	–	5.491	–	–	–	–	–	–	–
	DDBTS	–	–	–	–	4.676	–	–	–	–	–	–	–
	KD_1	–	$8.805e-04$	0.002	0.006	–	6.592	6.089	4.016	–	–	–	–
	KD_2	–	$8.805e-04$	0.002	0.006	–	6.592	6.089	4.016	–	–	–	–

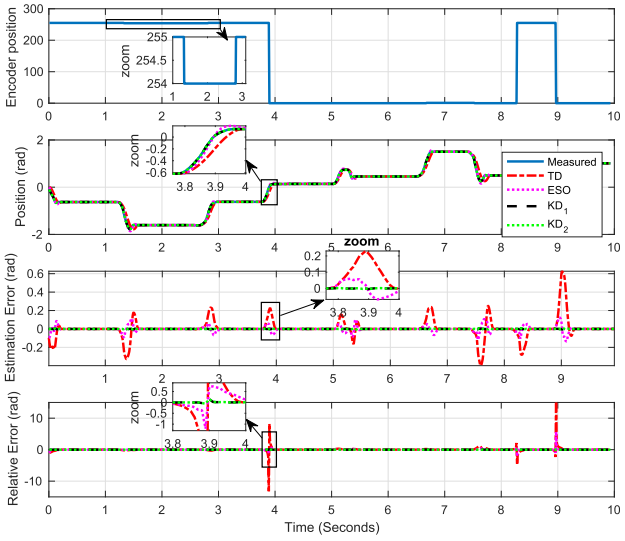

Fig. 6. Data acquisition of the rotor position with abrupt changes by QNET DCMCT, and its estimates with: TD, ESO, KD_1, and KD_2.

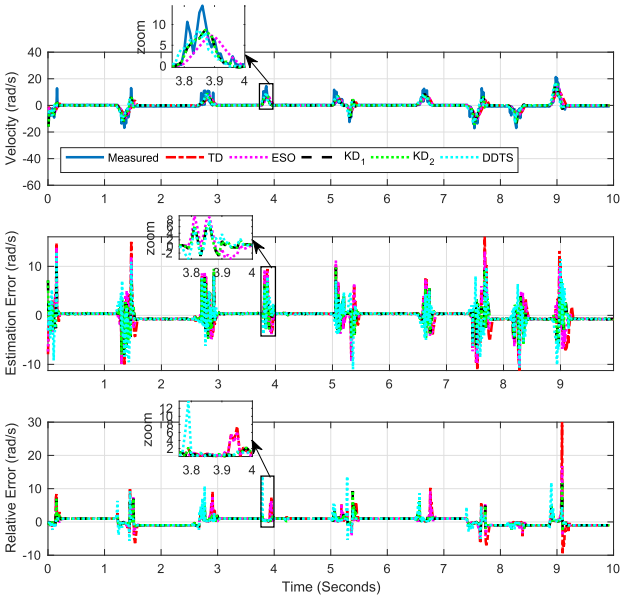

Fig. 7. Data acquisition of the rotor velocity by QNET DCMCT, (respect to Fig. 6) and its estimates with: TD, ESO, KD_1, KD_2, and DDBTS.

of the signals is not the purpose of this work but the improvement of its estimates.

In Table 1 are shown the percent error for the three test signals (the first signal is defined by (31) and the other signals were taken by DCMCT), where the proposed dynamical models KD_1 and KD_2 provides satisfactory estimates in position, velocity and acceleration. By the first signal test, the percent error was obtained respect to the ideal derivatives (32) and (33). In the measurement real signal, the percent error was obtained respect to the velocity provided by the tachometer included in DCMCT. The percent error was calculated by

$$\varepsilon_r = \frac{|x_i - x_v|}{x_v} \times 100\% \tag{34}$$

where x_i and x_v are the ideal and estimates values respectively.

In order to show the effect of the noise, the KD's are tested with different values of noise, as it can be seen in Table 1.

5. Conclusion

High accuracy estimates of instantaneous position, velocity and acceleration are obtained with the proposed algorithm (KD). The algorithm (KD) does not need a target velocity trajectory because its model is based on position measurements only. Also, the frequency of the signal is estimated and updated in the model step by step, making the filter more robust and expanding its operation range in speed. The proposed method is more effective than others because it can adapt to increases or decreases in sampling rate, that is an element of the proposed signal model. Furthermore, the proposed KD provides better estimates in signals with dynamic frequency. Signals were tested with smooth and abrupt changes in the position. The proposed algorithm provided the better results, except in the estimate of velocity when the signal present abrupt change, in its position. However, the estimates could be acceptable. This can be due to the model, that not contemplated abrupt changes because is based in an analytical function. On the other hand, note that KD makes it possible not only to estimate the position, velocity and acceleration but also its phasor. Furthermore using this method is more cost effective as it only needs a position measurement (one sensor, encoder) to obtain the velocity and acceleration estimates.

Appendix A

The elements of the matrix (11) are defined as

$$\lambda_{1,1} = 1, \quad \lambda_{1,2} = \tau, \quad \lambda_{1,3} = \frac{\tau^2}{2!}, \quad \cdots, \quad \lambda_{1,K} = \frac{\tau^K}{K!}$$

$$\lambda_{2,1} = j\omega, \quad \lambda_{2,2} = j\omega\tau + 1, \quad \lambda_{2,3} = (j\omega)\frac{\tau^2}{2!} + \tau$$

$$\lambda_{2,K} = j\omega\frac{\tau^K}{K!} + \frac{\tau^{K-1}}{(K-1)!}$$

$$\lambda_{3,1} = (j\omega)^2, \quad \lambda_{3,2} = (j\omega)^2\tau + 2j\omega$$

$$\lambda_{3,3} = (j\omega)^2\frac{\tau^2}{2!} + (2j\omega)\tau + 1$$

$$\lambda_{3,K} = (j\omega)^2\frac{\tau^K}{K!} + (2j\omega)\frac{\tau^{K-1}}{(K-1)!} + \tau$$

$$\lambda_{K,1} = (j\omega)^K, \quad \lambda_{K,2} = (j\omega)^K\tau + K(j\omega)^{K-1}$$

$$\lambda_{K,3} = (j\omega)^K\frac{\tau^2}{2!} + K(j\omega)^{K-1}\tau + K(K-1)j\omega$$

$$\lambda_{K,K} = (j\omega)^K\frac{\tau^K}{K!} + K(j\omega)^{(K-1)}\frac{\tau^{(K-1)}}{(K-1)!} + \ldots + 1$$

Appendix B. Supplementary data

Supplementary data associated with this article can be found, in the online version, at https://doi.org/10.1016/j.measurement.2019.05.043.

References

[1] K. Kim, J. Choi, J. Chung, G. Koo, I.-H. Bae, H. Sohn, Structural displacement estimation through multi-rate fusion of accelerometer and RTK-GPS displacement and velocity measurements, Measurement 130 (2018) 223–235, https://doi.org/10.1016/j.measurement.2018.07.090.

[2] S. Yu, Z. Shi, Dynamics of connected cruise control systems considering velocity changes with memory feedback, Measurement 64 (2015) 34–48, https://doi.org/10.1016/j.measurement.2014.12.036.

[3] X. Wei, F. Liu, L. Jia, Urban rail track condition monitoring based on in-service vehicle acceleration measurements, Measurement 80 (2016) 217–228, https://doi.org/10.1016/j.measurement.2015.11.033.

[4] F. Janabi-Sharifi, V. Hayward, C.S.J. Chen, Discrete-time adaptive windowing for velocity estimation, IEEE Trans. Control Syst. Technol. 8 (6) (2000) 1003–1009, https://doi.org/10.1109/87.880606.

[5] S. Valiviita, O. Vainio, Delayless differentiation algorithm and its efficient implementation for motion control applications, IEEE Trans. Instrum. Meas. 48 (5) (1999) 967–971, https://doi.org/10.1109/19.799655.

[6] O. Vainio, M. Renfors, T. Saramaki, Recursive implementation of FIR differentiators with optimum noise attenuation, IEEE Trans. Instrum. Meas. 46 (5) (1997) 1202–1207, https://doi.org/10.1109/19.676743.

[7] T. Burg, D. Dawson, Additional notes on the TORA example: a filtering approach to eliminate velocity measurements, IEEE Trans. Control Syst. Technol. 5 (5) (1997) 520–523, https://doi.org/10.1109/87.623037.

[8] R. Kelly, R. Ortega, A. Ailon, A. Loria, Global regulation of flexible joint robots using approximate differentiation, IEEE Trans. Autom. Control 39 (6) (1994) 1222–1224, https://doi.org/10.1109/9.293181.

[9] R.H. Brown, S.C. Schneider, M.G. Mulligan, Analysis of algorithms for velocity estimation from discrete position versus time data, IEEE Trans. Ind. Electron. 39 (1) (1992) 11–19, https://doi.org/10.1109/41.121906.

[10] A. Jaritz, M.W. Spong, An experimental comparison of robust control algorithms on a direct drive manipulator, IEEE Trans. Control Syst. Technol. 4 (6) (1996) 627–640, https://doi.org/10.1109/87.541692.

[11] P.R. Belanger, Estimation of angular velocity and acceleration from shaft encoder measurements, in: 1992 IEEE International Conference on Robotics and Automation, 1992. Proceedings, 1992, pp. 585–592 vol 1. doi:10.1109/ROBOT.1992.220228..

[12] S.B. Chang, M.H. Perng, State estimation from incremental sensor data corrupted by track miscounts and a detection delay, IEEE Trans. Control Syst. Technol. 4 (1) (1996) 65–71, https://doi.org/10.1109/87.481768.

[13] R. Gholipour, M.M. Fateh, Adaptive task-space control of robot manipulators using the Fourier series expansion without task-space velocity measurements, Measurement 123 (2018) 285–292, https://doi.org/10.1016/j.measurement.2018.04.003.

[14] W. Zhu, T. Lamarche, Velocity estimation by using position and acceleration sensors, IEEE Trans. Ind. Electron. 54 (5) (2007) 2706–2715, https://doi.org/10.1109/TIE.2007.899936.

[15] Y. Shao, D. Su, A. Al-Habaibeh, W. Yu, A new fault diagnosis algorithm for helical gears rotating at low speed using an optical encoder, Measurement 93 (2016) 449–459, https://doi.org/10.1016/j.measurement.2016.07.013.

[16] M. Rijnen, A. Saccon, H. Nijmeijer, Motion signals with velocity jumps: velocity estimation employing only quantized position data, IEEE Robot. Autom. Lett. 3 (3) (2018) 1498–1505, https://doi.org/10.1109/LRA.2018.2800097.

[17] J.F. Carneiro, F.G.D. Almeida, On the influence of velocity and acceleration estimators on a servopneumatic system behaviour, IEEE Access 4 (2016) 6541–6553, https://doi.org/10.1109/ACCESS.2016.2607284.

[18] B. Lotfi, L. Huang, An approach for velocity and position estimation through acceleration measurements, Measurement 90 (2016) 242–249, https://doi.org/10.1016/j.measurement.2016.04.011.

[19] K.V. Ramachandra, R.C. Division, Optimum steady state position, velocity, and acceleration estimation using noisy sampled position data, IEEE Trans. Aerosp. Electron. Syst. AES-23 (5) (1987) 705–708, https://doi.org/10.1109/TAES.1987.310865.

[20] J. Liu, F. Ni, P.A. Pegoraro, F. Ponci, A. Monti, C. Muscas, Fundamental and harmonic synchrophasors estimation using modified taylor-kalman filter, IEEE International Workshop on Applied Measurements for Power Systems (AMPS), 2012, pp. 1–6, https://doi.org/10.1109/AMPS.2012.6344004.

[21] J.Q. Han, W. Wang, Nonlinear tracking-differentiator, J. Syst. Sci. Math. Sci. 14 (2) (1994) 177–183.

[22] K.K. Tan, T.H. Lee, H.X. Zhou, Micro-positioning of linear-piezoelectric motors based on a learning nonlinear PID controller, IEE/ASME Trans. Mechatronics 6 (4) (2001) 428–436, https://doi.org/10.1109/3516.974856.

[23] Y.X. Su, B.Y. Duan, C.H. Zheng, Y.F. Zhang, G.D. Chen, J.W. Mi, Disturbance-rejection high-precision motion control of a stewart platform, IEEE Trans. Control Syst. Technol 12 (3) (2004) 364–374, https://doi.org/10.1109/TCST.2004.824315.

[24] H. Jingqing, The extended state observer of a class of uncertain systems, Control Decision 10 (1) (1995) 85–88.

[25] B.-Z. Guo, Z.-L. Zhao, Extended state observer for nonlinear systems with uncertainty, IFAC Proc. 44 (1) (2011) 1855–1860, https://doi.org/10.3182/20110828-6-IT-1002.00399, URL: http://www.sciencedirect.com/science/article/pii/S1474667016438802.

[26] I.R. Khan, R. Ohba, New design of full band differentiators based on taylor series, IEE Proc. – Vision, Image Signal Process. 146 (4) (1999) 185–189, https://doi.org/10.1049/ip-vis:19990380.

[27] Y.X. Su, C.H. Zheng, P.C. Mueller, B.Y. Duan, A simple improved velocity estimation for low-speed regions based on position measurements only, IEEE Trans. Control Syst. Technol. 14 (5) (2006) 937–942, https://doi.org/10.1109/TCST.2006.876917.

[28] K.K.C. Yu, N.R. Watson, J. Arrillaga, An adaptive Kalman filter for dynamic harmonic state estimation and harmonic injection tracking, IEEE Trans. Power Delivery 20 (2) (2005) 1577–1584, https://doi.org/10.1109/TPWRD.2004.838643.